M. Elias-Espinosa, M. Keddam*, M. Ortiz-Domínguez, A. Arenas-Flores, J. Zuno-Silva, F. Cervantes-Sodi and J. A. Reyes-Retana

Investigation of Growth Kinetics of Fe_2B Layers on AISI 1518 Steel by the Integral Method

https://doi.org/10.1515/htmp-2017-0166
Received November 08, 2017; accepted June 29, 2018

Abstract: The AISI 1518 steel was pack-borided in the temperature range 1123–1273 K for a treatment ranging from 2 to 8 h. A compact single boride layer (Fe_2B) was formed at the surface of the AISI 1518 steel using the mixture of powders composed of 20 % B_4C, 10 % KBF_4 and 70 % SiC. The following experimental techniques such as scanning electron microscopy coupled with EDS analysis and X-ray diffraction analysis were employed to characterize the pack-borided AISI 1518 steel. An alternative model, based on the integral mass balance equation, was used to estimate the boron diffusion coefficients in the Fe_2B layers in the temperature range 1123–1273 K. Finally, the value of activation energy for boron diffusion in the AISI 1518 steel was estimated and compared with the literature data. Furthermore, the present model was validated by comparing the experimental value of Fe_2B layer thickness, obtained at 1253 K for 2 h of treatment, with the predicted value.

Keywords: incubation time, iron boride, growth kinetics, activation energy, integral method

***Corresponding author: M. Keddam,** Laboratoire de Technologie des Matériaux, Faculté de Génie Mécanique et Génie des Procédés, USTHB, B.P. No. 32, 16111 El-Alia, Bab-Ezzouar, Algiers, Algeria, E-mail: keddam@yahoo.fr
M. Elias-Espinosa, Instituto Tecnológico y de Estudios Superiores de Monterrey-ITESM Campus Santa Fe, Av. Carlos Lazo No. 100, Del. Álvaro Obregón, CP. 01389, México City, México, E-mail: mielias@itesm.mx
M. Ortiz-Domínguez, Universidad Autónoma del Estado de Hidalgo, Escuela Superior de Ciudad Sahagún-Ingeniería Mecánica, Carretera Cd. Sahagún-O tumba s/n, Zona Industrial CP. 43990, Hidalgo, México, E-mail: martin_ortiz@uaeh.edu.mx
A. Arenas-Flores, Centro de Investigaciones en Materiales y Metalurgia, Universidad Autónoma del Estado de Hidalgo, Ciudad Universitaria Pachuca-Tulancingo km. 4.5, Pachuca, Hidalgo, México, E-mail: arenasa@uaeh.edu.mx
J. Zuno-Silva, Universidad Autónoma del Estado de Hidalgo, Escuela Superior de Ciudad Sahagún-Ingeniería Mecánica, Carretera Cd. Sahagún-O tumba s/n, Zona Industrial CP. 43990, Hidalgo, México, E-mail: zunojorge@gmail.com
F. Cervantes-Sodi, Departamento de Física y Matemáticas, Universidad Iberoamericana Ciudad de México, Prolongación Paseo de la Reforma 880, Lomas de Santa Fe, CP. 01219, México City, México, E-mail: felipe.cervantes@ibero.mx
J. A. Reyes-Retana, Instituto Tecnológico y de Estudios Superiores de Monterrey-ITESM Campus Santa Fe, Av. Carlos Lazo No. 100, Del. Álvaro Obregón, CP. 01389, México City, México; Departamento de Física y Matemáticas, Universidad Iberoamericana Ciudad de México, Prolongación Paseo de la Reforma 880, Lomas de Santa Fe, CP. 01219, México City, México, E-mail: jareyesretana@itesm.mx

Introduction

The boriding process is a thermochemical treatment involving a chemical modification of surfaces of treated parts with the purpose of increasing their tribological properties and corrosion resistance [1]. This thermochemical process, used to form iron borides, is carried out in the temperature range 700–1000 °C depending on the boriding media used [2–7]. This process results in the formation of a wear-resistant iron boride layer on the surface of steel parts by thermodiffusion. The boride layer is either a single-phase layer (Fe_2B) or a double-phase layer with FeB and Fe_2B. For industrial applications, the monolayer configuration (Fe_2B) is preferred to the bilayer configuration (FeB and Fe_2B) since FeB, is harder and brittle than Fe_2B, and having a large coefficient of thermal expansion. As a consequence, cracks can form and propagate along the (FeB/Fe_2B) interface because of the high hardness of FeB. Many boriding methods exist for producing wear-resistant boride layers including different media (solid, liquid, gas, and plasma). However, the powder-pack-boriding presents some important advantages such as: easy handling, the possibility of modifying the composition of the boriding agent, minimal equipment, and cost-effectiveness.

From a kinetic viewpoint, several models dealing with the growth kinetics of boride layers on different substrates were reported in many research papers [8–17].

For example, the authors VillaVelázquez-Mendoza et al. [8]. have used the response surface methodology for studying the evolution of boride layers produced by paste-boriding on the AISI 1018 steel in the temperature range 1073–1273 K as a function of temperature, time and substrate roughness. Based on the ANOVA analysis, the boriding temperature had the highest contribution on the boride layer thickness.

The authors Campos et al. [9] have employed the neural network and the least square models in order to investigate the boriding kinetics of AISI 1045 steel. In this research paper, a single boride phase (Fe_2B) layer was produced by the paste-boriding process in the temperature range 1193–1273 K, by modifying the boron paste thickness. These two approaches have been experimentally validated for the samples borided at 1223 K for 5 h of treatment by varying the value of boron paste thickness of 2–5 mm. The technique of fuzzy logic was also employed by Campos et al. [10]. to investigate the growth kinetics of Fe_2B layers at the surface of AISI 1045 steel by the paste-boriding treatment. The experimental results in terms of boride layer thickness were compared with those provided by the technique of fuzzy logic and a satisfactory agreement was observed between these two set of data. It is concluded that the utilization of fuzzy logic approach constitutes an alternative for the modelling the growth kinetics of boride layers. The phase-field model has been applied by Ramdan et al. [11]. to simulate the boron-concentration profile through the Fe_2B layers formed on Armco iron based on the experimental data taken from the reference work [10]. This kinetic approach was derived from Ginzburg-Landau free energy functional that uses the thermodynamic data of Fe–B phase diagram and the following physical parameters of the material (interface energy and interface thickness). The Fe_2B phase was assumed to be stoichiometric during the formulation of phase-field model.

Campos et al. [12]. have used a simple diffusion model based on the kinetic model developed by Brakman et al. [13]. The model considered the principle of mass conservation at the (Fe_2B/substrate) interface during the formation of Fe_2B layers on Armco-iron by ignoring the effect of boride incubation times and taking into account the difference in molar volume between the Fe_2B phase and the substrate. A linear boron-concentration profile through the Fe_2B layer was assumed for estimating the diffusion coefficient of boron in Fe_2B in the temperature range 1223–1323 K.

Recently, Gómez-Vargas et al. [14]. have suggested a mathematical model for investigating the growth kinetics of Fe_2B layers on AISI 1025 steel in the temperature range 1123–1273 K. This kinetic model was based on the principle of mass conservation at the (Fe_2B/substrate) interface. A non-linear boron-concentration profile that satisfies the solution of Second Fick's law was considered. For solving this diffusion problem, a non dimensional kinetic parameter was introduced where the boride incubation time for the formation of Fe_2B layers was independent of the boriding temperature.

Mebarek et al. [15]. have used a diffusion model for predicting the boride incubation times during the formation Fe_2B layers on XC 38 steel based on solving the mass balance equation at the (Fe_2B/substrate) interface and by using the concept of surface boron concentration instead of upper and lower limits for boron concentration in Fe_2B.

These different approaches can be used to select the optimum boride layers' thicknesses according to the industrial applications of the borided materials.

The aim of this present work was to characterize the Fe_2B layers formed on AISI 1518 steel and to investigate its boriding kinetics.

For this purpose, an alternative diffusion model based on the integral method was suggested [16, 17] to investigate the kinetics of formation of Fe_2B layers on AISI 1518 steel. The present model assumes a non-linear boron-concentration profile through the Fe_2B layer with an occurrence of boride incubation time. As an advantage compared to other models, a simple equation was obtained that relates the diffusion coefficient of boron in Fe_2B to the square of parabolic growth constant at the (Fe_2B/substrate) interface. By using this equation, the boron diffusion coefficients in Fe_2B and the value of activation energy for boron diffusion in AISI 1518 steel were estimated in the temperature range 1123–1273 K. Finally, an experimental validation of the present diffusion model was made by using an extra boriding condition (1253 K for 2 h).

The diffusion model

The diffusion model considers the growth of a single boride layer (Fe_2B) over a saturated substrate with boron atoms of AISI 1518 steel Schematic boron concentration – profile through the Fe_2B layer is displayed in Figure 1. The $f(x,t)$ function gives the distribution of boron concentration in the substrate before the nucleation of Fe_2B phase. $t_0^{Fe_2B}(T)$ is the incubation time required to get a compact layer of Fe_2B. $C_{up}^{Fe_2B}$ represents the upper limit of boron content in Fe_2B ($= 9$ wt.%) while $C_{low}^{Fe_2B}$ is the lower limit of boron content in Fe_2B ($= 8.83$ wt.%). The point $x(t) = u$ is the Fe_2B layer thickness or the position of (Fe_2B/substrate) interface. A small homogeneity range of about 1 at. % was reported for the Fe_2B layer [13]. The term C_{ads}^{B} is the adsorbed boron concentration in the boride layer during the boriding treatment [18]. C_0 is the boron solubility in the matrix which is very low (≈ 0 wt.%)[19, 20].

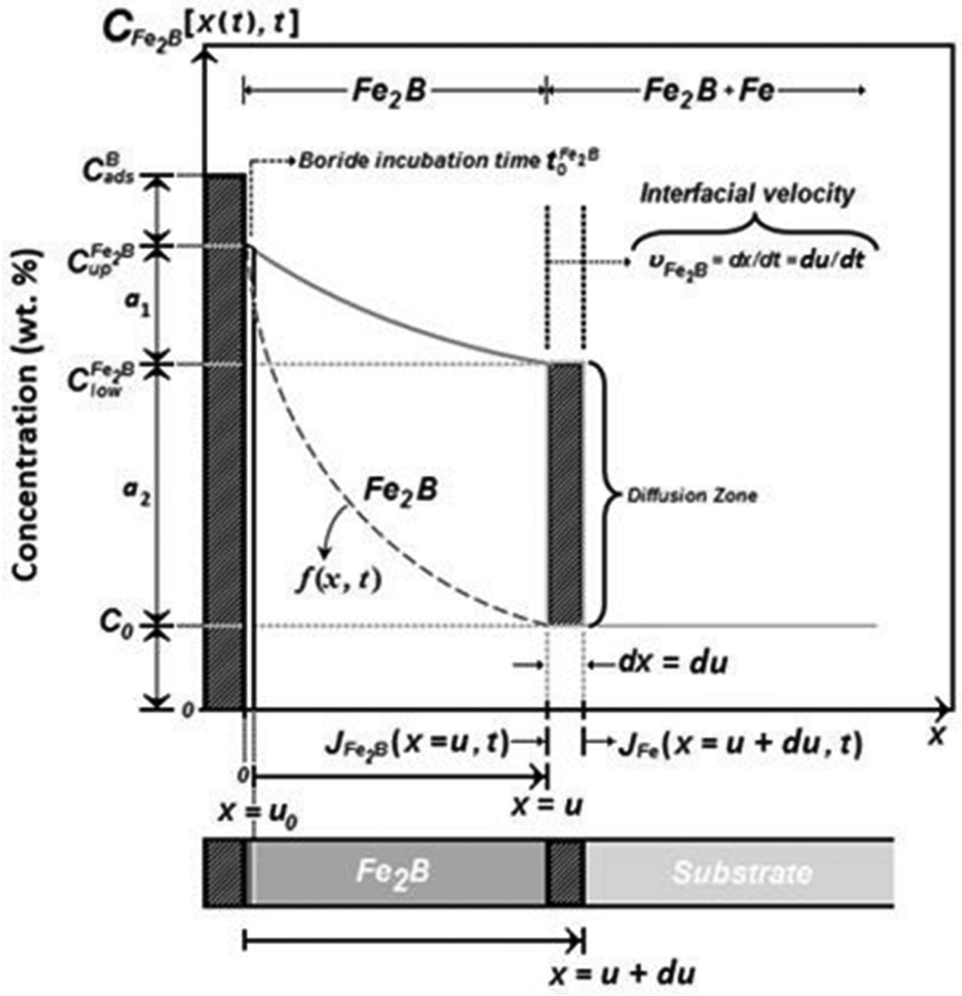

Figure 1: Schematic representation of the boron-concentration profile through the Fe_2B layer.

The following assumptions are considered during the formulation of the diffusion model:

- The growth kinetics is controlled by the boron diffusion in the Fe_2B layer.
- The Fe_2B phase nucleates after a specific incubation time.
- The boride layer grows because of the boron diffusion perpendicular to the specimen surface.
- Boron concentrations remain constant in the boride layer during the treatment.
- The boride layer is thin compared to the sample thickness.
- A uniform temperature is assumed throughout the sample.
- Planar morphology is assumed for the phase interface.

The initial and boundary conditions for the diffusion problem are given by

$$t = 0,\ x > 0,\ \text{with}\ C_{Fe_2B}[x(t),\ t = 0] = C_0 \approx 0 \quad \text{wt.\%} \tag{1}$$

Boundary conditions:

$$C_{Fe_2B}[x(t = t_0^{Fe_2B}) = 0, t = t_0] = C_{up}^{Fe_2B} \text{ for } C_{ads}^{B} > 8.83\,\text{wt.\%} \tag{2}$$

$$C_{Fe_2B}[x(t = t) = u(t),\ t = t] = C_{low}^{Fe_2B}\ for\ C_{ads}^{B} < 8.83\,\text{wt.\%} \tag{3}$$

The Second Fick's law that describes the evolution of boron concentration in Fe_2B as a function of diffusion distance x(t) and time t is expressed by eq. (4):

$$D_{Fe_2B}\frac{\partial^2 C_{Fe_2B}[x, t]}{\partial x^2} = \frac{\partial C_{Fe_2B}[x, t]}{\partial t} \tag{4}$$

where the boron diffusion coefficient is only dependent on the boriding temperature. The expression of boron-concentration profile through the Fe_2B layer was adopted from the Goodman's method [21].

$$C_{Fe_2B}[x,t] = C_{low}^{Fe_2B} + a(t)(u(t)-x) + b(t)(u(t)-x)^2 \text{ for } 0 \le x \le u \tag{5}$$

The three time-dependent unknowns $a(t)$, $b(t)$, and $u(t)$ must satisfy the boundary conditions given by eqs. (2) and (3). It is noticed that the two parameters $a(t)$ and $b(t)$ must be positive because of a decreasing nature of the concentration profile of boron element. By applying the boundary condition on the surface, eq. (6) was obtained:

$$a(t)u(t) + b(t)u(t)^2 = (C_{up}^{Fe_2B} - C_{low}^{Fe_2B}) \tag{6}$$

By integrating eq. (4) between 0 and $u(t)$ and applying the Leibniz rule, the ordinary differential equation (ODE) given by eq. (7) was obtained:

$$\frac{u(t)^2}{2}\frac{da(t)}{dt} + a(t)u(t)\frac{du(t)}{dt} + \frac{u(t)^3}{3}\frac{db(t)}{dt} + b(t)u(t)^2\frac{du(t)}{dt} = 2D_{Fe_2B}b(t)u(t) \tag{7}$$

The mass balance equation at the (Fe_2B/substrate) interface is given by eq. (8):

$$W\frac{dx}{dt}\bigg|_{x=u} = -D_{Fe_2B}\frac{\partial C_{Fe_2B}[x,t]}{\partial x}\bigg|_{x=u} \tag{8}$$

with $W = [\frac{(C_{up}^{Fe_2B} - C_{low}^{Fe_2B})}{2} + (C_{low}^{Fe_2B} - C_0)]$

At the (Fe_2B/substrate) interface, the boron concentration remains constant and eq. (8) can be rewritten as follows:

$$W\left(-\frac{\frac{\partial C_{Fe_2B}[x,t]}{\partial t}\Big|_{x=u}}{\frac{\partial C_{Fe_2B}[x,t]}{\partial x}\Big|_{x=u}}\right) = -D_{Fe_2B}\frac{\partial C_{Fe_2B}[x,t]}{\partial x}\bigg|_{x=u} \tag{9}$$

Substituting eq. (4) into eq. (9) and after derivation with respect to the diffusion distance x(t), eq. (10) was obtained:

$$(C_{up}^{Fe_2B} + C_{low}^{Fe_2B})b(t) = a(t)^2 \tag{10}$$

Equations (6), (7) and (10) form a set of differential algebraic equations (DAE) in $a(t)$, $b(t)$, and $u(t)$ subjected to the initial conditions of this diffusion problem. To determine the expression of boron diffusion coefficient in the Fe_2B layers, an analytic solution exists for this diffusion problem by setting:

$$u(t) = k[t - t_0^{Fe_2B}(T)]^{1/2} \tag{11}$$

$$a(t) = \frac{\alpha}{u(t)} \tag{12}$$

and

$$b(t) = \frac{\beta}{u(t)^2} \tag{13}$$

where $u(t)$ is the Fe_2B layer thickness, $t_0^{Fe_2B}(T)$ the associated incubation time and k the parabolic growth constant at the (Fe_2B/substrate) interface. It is noticed that the use of eq. (11) is acceptable from a practical point of view since it has been observed in many experiments. The two unknowns α and β have to be identified for solving this diffusion problem. After substitution of eqs. (11), (12) and (13) into the DAEs system and derivation, the expression of boron diffusion coefficient was obtained as follows:

$$D_{Fe_2B} = \eta k^2 \tag{14}$$

with $\eta = [(\frac{1}{16})(\frac{C_{up}^{Fe_2B} + C_{low}^{Fe_2B}}{C_{up}^{Fe_2B} - C_{low}^{Fe_2B}})(1 + \sqrt{1 + 4(\frac{C_{up}^{Fe_2B} - C_{low}^{Fe_2B}}{C_{up}^{Fe_2B} + C_{low}^{Fe_2B}})}) + (\frac{1}{12})]$

along with the expressions of a(t) and b(t) given by eqs. (15) and (16):

$$a(t) = \frac{\alpha}{k[t - t_0^{Fe_2B}(T)]^{1/2}} \tag{15}$$

$$b(t) = \frac{\beta}{k^2[t - t_0^{Fe_2B}(T)]} \tag{16}$$

with $\alpha = \frac{(C_{up}^{Fe_2B} + C_{low}^{Fe_2B})}{2}[-1 + \sqrt{1 + 4(\frac{C_{up}^{Fe_2B} - C_{low}^{Fe_2B}}{C_{up}^{Fe_2B} + C_{low}^{Fe_2B}})}]$
and $\beta = \frac{\alpha^2}{(C_{up}^{Fe_2B} + C_{low}^{Fe_2B})}$

Experimental details

The material and the boriding treatment

The material to be pack- borided was AISI 1518 steel. The chemical composition of AISI 1518 steel is given (in weight percent) in Table 1. The samples had a cubic shape with dimensions of 10mm × 10mm × 10mm. Prior to the boriding process, the samples were polished, ultrasonically cleaned in an alcohol solution and deionized water for 15 min at room temperature, and dried and stored under clean-room conditions. Afterwards, the samples were embedded in a closed, cylindrical case in contact with a mixture of powders consisting of 20 % B_4C, 10 % KBF_4 and 70 % SiC. The powder-pack boriding process was carried out in a conventional furnace under a pure argon atmosphere in the temperature range 1123–1223 K. Four treatment times (2, 4, 6, and 8 h) were selected for each temperature. Once the boriding treatment was finished the container was removed from the furnace and slowly cooled to room temperature.

Table 1: The chemical composition of AISI 1518 steel (in weight percent).

C	Si	Mn	P	S	Fe
0.15–0.21	0.20–0.40	1.10–1.40	0.040	0.050	Balance

Experimental techniques

The borided and etched samples were cross-sectioned for microstructural investigations using a LECO VC-50 cutting precision machine and the cross-sections of formed boride layers were observed by SEM (JEOL JSM 6300 LV). For a kinetic study, the boride layer thickness was automatically measured with the aid of MSQ PLUS *software*. To ensure the reproducibility of the measured layers, seventy measurements were taken from different sections of the borided samples to estimate the Fe_2B layer thickness; defined as an average value of the long boride teeth [22]. The boride formed on the surface of borided sample was identified by means of X-Ray Diffraction (XRD) equipment (Equinox 2000) using CoK_α radiation at $\lambda = 0.179$ nm.

Results and discussion

SEM observations and EDS analysis

Figure 2 gives the SEM micrographs of cross-sections of Fe_2B layers formed at the surfaces of AISI 1518 steel borided at 1173 K for increasing treatment times. The obtained boride layers look dense and compact exhibiting a saw-tooth morphology for all boriding conditions. This particular morphology promotes a good adhesion to the substrate [23]. The thickness of Fe_2B layer increased with the change in the boriding temperature because the diffusion phenomenon of boron atoms into the substrate is a thermally activated process. The value of Fe_2B layer thickness ranged from 55.8 ± 10.5 µm for 2 h of treatment to 149.3 ± 22.5 µm for 8 h at 1173 h.

The EDS analysis was carried out at the surface of borided sample and in the vicinity of the (boride layer/substrate) interface as shown in Figure 3. Figure 3 **(a)** indicated the presence of iron element with boron element. At the surface of borided sample, the iron atoms combine with the boron atoms to form the Fe_2B phase by a mechanism of nucleation and growth of Fe_2B crystals. Figure 3 **(b)** showed an EDS analysis in the vicinity of the (Fe_2B/substrate) interface where the following elements: iron, carbon, silicon and manganese are present. Carbon and silicon are diffused towards the diffusion zone to form together with boron, solid solutions as silicoborides ($FeSi_{0.4}B_{0.6}$ and Fe_5SiB_2) and boroncementite ($Fe_3B_{0.67}C_{0.33}$) [24].

X-ray diffraction analysis

Figure 4 gives the XRD pattern obtained at the surface of pack-borided AISI 1518 steel at 1273 K during 8 h. The XRD pattern revealed the existence of Fe_2B layer over the surface of AISI 1518 steel. The diffraction peaks showed a difference in intensities that depends on the crystallographic orientations of Fe_2B crystals. Furthermore, the growth of Fe_2B layer is if a highly anisotropic nature [25].

Growth kinetics of Fe_2B layers

The diffusion model requires the kinetic data to estimate the values of boron diffusion coefficients in the Fe_2B layers in the temperature range 1123–1273 K by using eq. (14).

Figure 5 describes the evolution of the square of Fe_2B layer thickness versus the treatment time for different boriding temperatures.

Table 2 gives the experimental values of parabolic growth constants at the (Fe_2B/substrate) interface along with the corresponding boride incubation times deduced from Figure 5. These data were obtained by plotting the square of Fe_2B layer thickness versus time according to eq. (11). In addition, it is noticed that the boride incubation time is independent on the boriding temperature.

Figure 6 gives the temperature dependence of boron diffusion coefficients through the Fe_2B layers according to Arrhenius relationship. The expression of boron diffusion coefficient in the Fe_2B layer can be readily obtained using a linear fitting in the temperature range 1123–1273 K:

$$D_{Fe_2B} = 1.0107 \times 10^{-4} \exp\left[\frac{-(160.45 \pm 5.7) kJmol^{-1}}{RT}\right] \quad (17)$$

where $R = 8.314$ J mol^{-1} K^{-1} and T the absolute temperature in Kelvin.

Table 3 compares the value of activation energy for boron diffusion in AISI 1518 steel with the values of activation energy reported in the literature data for some borided materials (Armco iron and steels) [7, 12, 26–30]. It is noticed that the published values of activation energy for boron diffusion depended on various factors such as: (the

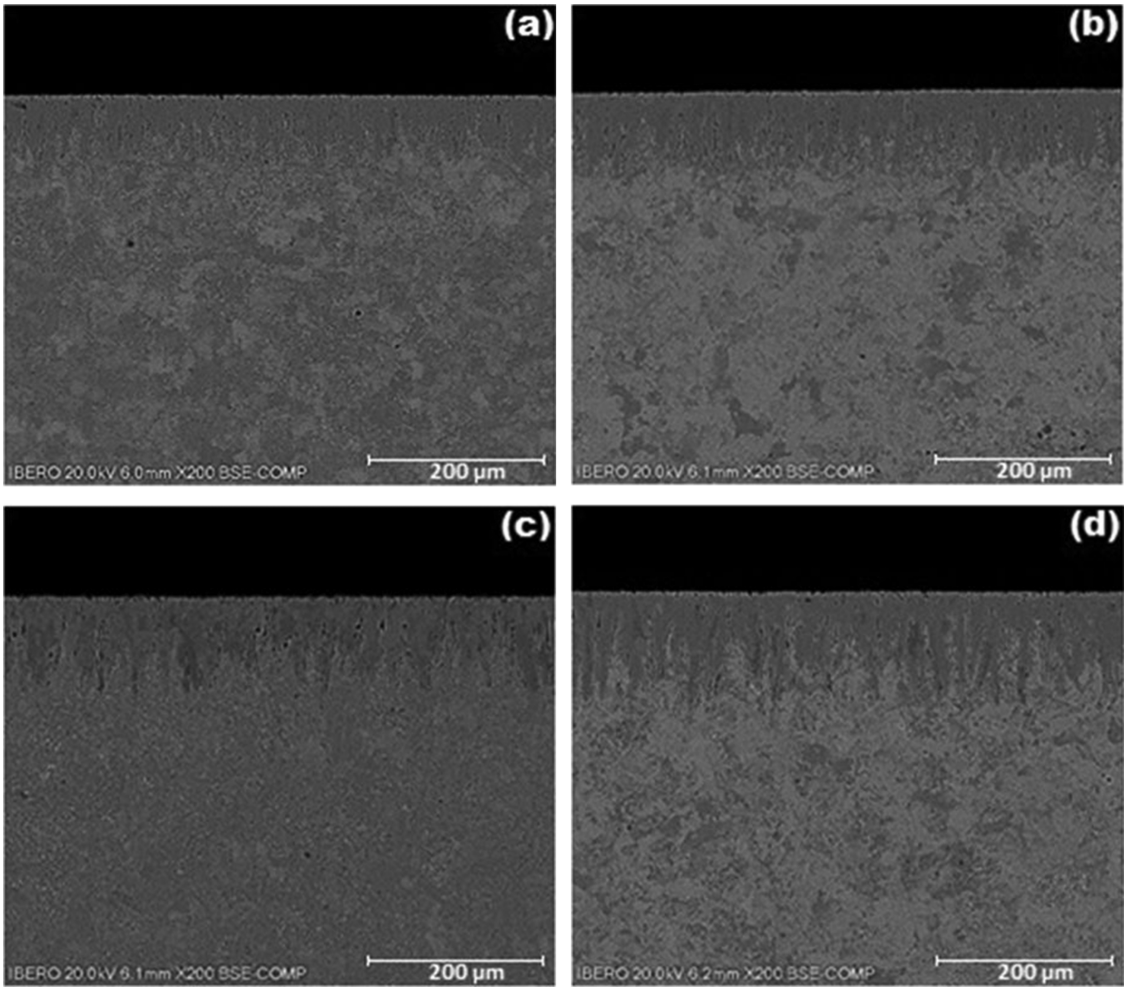

Figure 2: SEM micrographs of the cross-sections of AISI 1518 steels borided at 1173 K during different exposure times: (a) 2 h, (b) 4 h, (c) 6 h, and (d) 8 h.

temperature range considered, the boriding method, the chemical composition of treated material, the method of calculation and mechanism of boron diffusion). The observed differences in the values of activation energies for boron diffusion in the treated materials indicate that the rate-determining steps in powder and paste-boriding deviate from that for plasma paste-boriding and that for gas boriding process [7, 12, 14, 26]. In the work carried out by Altinsoy et al [30].,The obtained value of activation energy for boron diffusion in AISI 1020 steel was very comparable with that found in this work (= 160.45 ± 5.7 kJ mol^{-1}) for AISI 1518 steel. This value of activation energy for boron diffusion was interpreted as the amount of energy for the movement of boron atoms in the easier path for the boron diffusion in the body centred tetragonal lattice of Fe_2B that minimizes the growth stresses [25]. Regarding the nature of boride coatings, Palombarini et Carbucicchio [31] reported that the saw-tooth morphology of the (boride layer/substrate) interface in low alloy steels can be explained by enhanced growth at the tips of boride needles.

In the present study, the SEM observations revealed that many of borided needles are of dentritic nature as reported by Ninham and Hutchings [32]. The columnar nature of this interface is resulting from the side arm growth similar to that observed during the solidification of metallic alloys or metals [33].

Experimental verification of the diffusion model

The validity of this diffusion model was verified by a comparison of experimental value of Fe_2B layer thickness obtained at 1253 K during 2 h of treatment with the predicted value of Fe_2B layer thickness given by eq. (18).

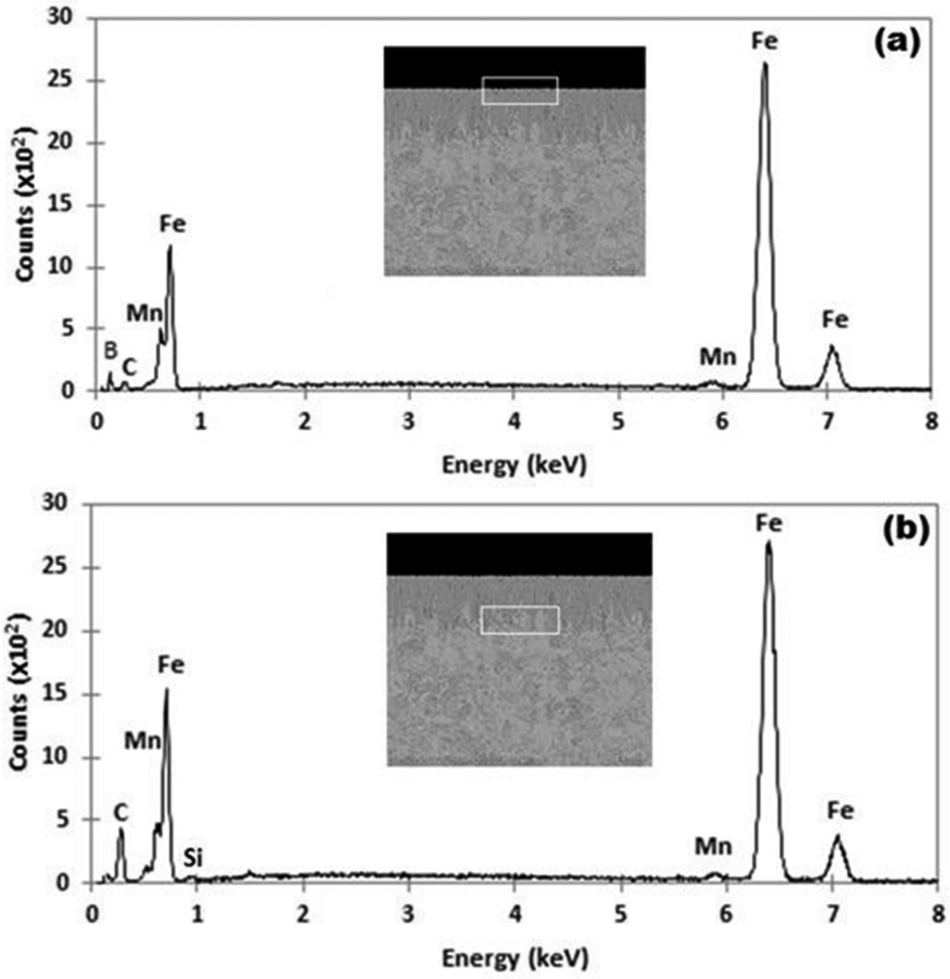

Figure 3: EDS spectra on the SEM micrograph of the cross-section of borided AISI 1518 steel at 1173 K for 8 h. (a) EDS spectrum obtained at the surface, (b) EDS spectrum obtained at the (Fe_2B/substrate) interface.

$$u(t) = \sqrt{\frac{D_{Fe_2B}[t - t_0^{Fe_2B}(T)]}{\eta}} \tag{18}$$

with $\eta = 13.3175$

Figure 7 shows the SEM micrograph of the cross-section of the sample borided at 1253 K for 2 h. Table 4 shows a comparison between the experimental value of Fe_2B layer thickness obtained at 1253 K for 2 h and the predicted value given by eq. (18) for an upper boron content in the Fe_2B phase equal to 9 wt.%. Therefore, the predicted value of Fe_2B layer thickness agree with the data obtained experimentally, From a practical point of view, and for this kind of steel, knowledge of the variables that control the boriding treatment is of great importance for obtaining the optimum value of Fe_2B layer thickness.

Conclusions

In the present work, the AISI 1518 steel was subjected to the pack-boriding process in the mixture of powders composed of (20 % B_4C, 10 % KBF_4 and 70 % SiC) in the temperature range 1123–1223 K for a variable treatment between 2 and 8 h. A monolayer configuration (Fe_2B) was seen in all SEM micrographs exhibiting a saw-toothed morphology. The crystalline nature of this iron boride was confirmed by XRD analysis. The growth kinetics of Fe_2B layers followed a parabolic growth law. A particular solution of a system of DAEs has been obtained in order to estimate the boron diffusion coefficients in the Fe_2B layers in the temperature range 1123–1273 K. On the basis of our experimental data, the value of activation energy for boron diffusion was estimated as 160.45 ± 5.7 kJ mol^{-1} for AISI 1518 steel. This value of energy is needed to

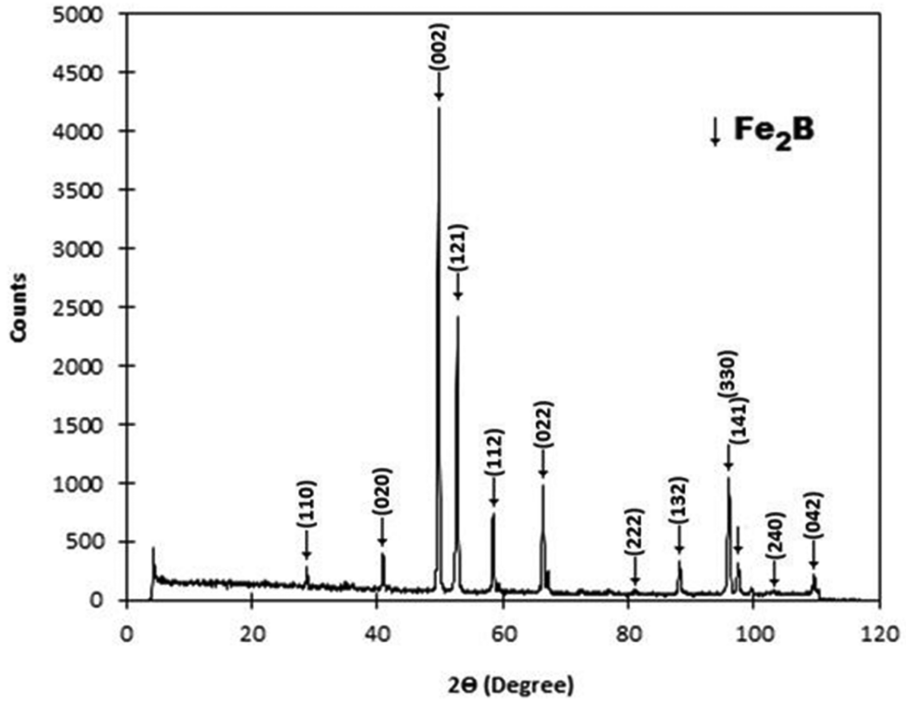

Figure 4: XRD pattern obtained at the surface of the borided AISI 1518 steel at 1273 K for 8 h.

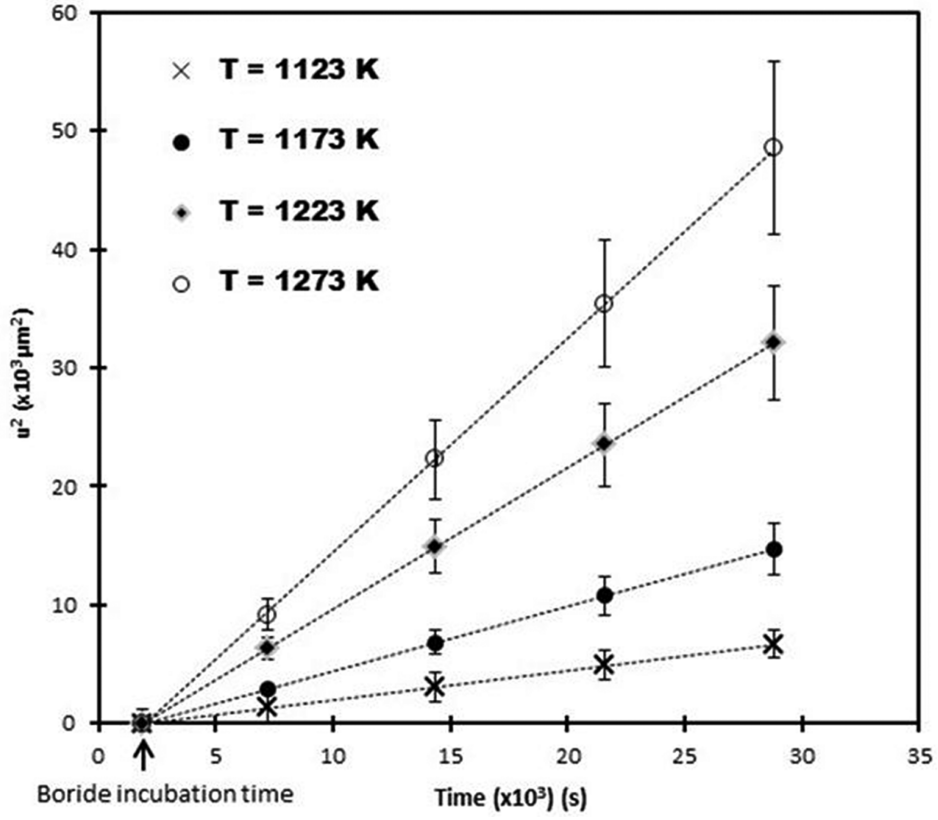

Figure 5: Square of Fe_2B layer thickness as a function of boriding time at increasing temperatures.

Table 2: The experimental values of parabolic growth constants at the (Fe_2B/substrate) interface along with the corresponding boride incubation times.

T(K)	Experimental parabolic growth constant k $(\mu m \cdot s^{-0.5})$	Boride incubation time $t_0^{Fe_2B}(T)$ (s)
1123	0.5000	2025
1173	0.7416	2025
1223	1.0909	2025
1273	1.3491	2025

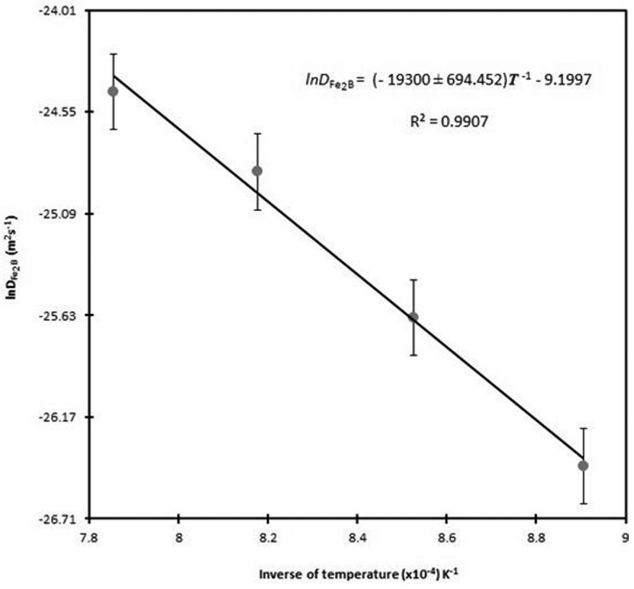

Figure 6: Temperature dependence of the boron diffusion coefficient in Fe_2B.

overcome the energetic barrier for activating the boron diffusion along the preferred crystallographic direction [100]. In addition, the present diffusion model was also verified experimentally for the sample borided at 1253 K for 2 h. A good agreement was observed between the experimental result and the predicted value of Fe_2B layer thickness.

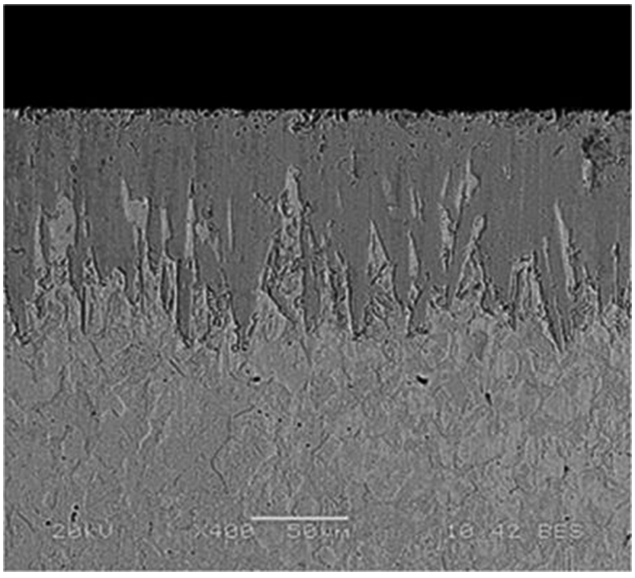

Figure 7: SEM micrograph of Fe_2B layer formed on AISI 1518 steel at 1253 K for 2 h.

Table 4: Comparison between the experimental value of Fe_2B layer thickness obtained at 1253 K for 2 h and the predicted value using the integral method for an upper boron content in the Fe_2B phase equal to 9 wt.%.

Boriding conditions	Experimental Fe_2B layer thickness (μm)	Simulated Fe_2B layer thickness (μm) by eq. (18)
1253 K for 2 h	102.6 ± 12.2	89.6

List of symbols

$u(t)$ is the Fe_2B layer thickness (μm).
a(t) and b(t) are the time-dependent parameters

Table 3: Comparison of activation energy for boron diffusion in AISI 1518 steel with other borided materials (Armco iron and steels).

Material	Boriding method	Activation energy (kJ mol $^{-1}$)	Temperature range (K)	References
Armco iron	Gaseous	87.857 (FeB) 117.508 (Fe_2B)	1073–1273	[26]
Armco iron	Paste	151 (Fe_2B)	1223–1323	[12]
AISI 1018 steel	Electrochemical	172.75 ± 8.6 (FeB + Fe_2B)	1123–1273	[27]
AISI 440C steel	Plasma paste-boriding	134.62 (FeB + Fe_2B)	973–1073	[7]
AISI 304 steel	Salt bath	253 0.35 (FeB + Fe_2B)	1073–1223	[28]
AISI P20 steel	Pack- powder	200 (FeB + Fe_2B)	1073–1223	[29]
AISI 1020 steel	Pack- powder	164.356 (Fe_2B)	1073–1223	[30]
AISI 1518 steel	Pack- powder	160.4 5 ± 5.7 (Fe_2B)	1123–1273	This work

k is the parabolic growth constant of the Fe_2B layer ($\mu ms^{-0.5}$).
t is the treatment time (s).
$t_0^{Fe_2B}(T)$ is the boride incubation time (s).
$C_{up}^{Fe_2B}$ represents the upper limit of boron content in Fe_2B (= 9 wt.%).
$C_{low}^{Fe_2B}$ is the lower limit of boron content in Fe_2B (= 8.83wt.%).
C_{ads}^{B} is the adsorbed boron concentration in the boride layer (wt..%).
C_0 is the boron solubility in the matrix ($\approx$ 0 wt.%).
$C_{Fe_2B}[x,t]$ is the boron concentration profile in the layer (Fe_2B wt.%).
D_{Fe_2B} represents the diffusion coefficient of boron in the Fe_2B phase ($m^2\ s^{-1}$).

Acknowledgements: The work described in this paper was supported by a grant of PRDEP and CONACyT México. Likewise, FCS reconoce los fondos del Departamento de Física y Matemáticas y de la División de Investigación de la UIA. The authors wish to thank the Laboratorio de Microscopía de la UIA.

References

[1] A.K. Sinha, J. Heat Treat., 4 (1991) 437–447.
[2] K.S. Nam, K.H. Lee, S.R. Lee and S.C. Kwon, Surf. Coat. Technol., 98 (1998) 886–890.
[3] E.A. Smol'nikov and L.M. Sarmanova, Met. Sci. Heat Treat., 24 (1982) 785–788.
[4] N.N. Mitrokhovich, V.P. Fetisov and N.N. Lipchin, Met. Sci. Heat Treat., 24 (1982) 415–417.
[5] A.N. Simonenko, V.A. Shestakov and V.N. Poboinya, Met. Sci. Heat Treat., 24 (1982) 360–361.
[6] I. Gunes and M. Ozcatal, Mater. Technol., 49 (2015) 759–763.
[7] M. Keddam, R. Chegroune, M. Kulka, D. Panfil, S. Ulker and S. Taktak, Trans. Indian Inst. Met, 70 (2017) 1377–1385.
[8] C.I. VillaVelázquez-Mendoza, J.L. Rodríguez-Mendoza, V. Ibarra-Galván, R.P. Hodgkins, A. López-Valdivieso, L.L. Serrato-Palacios, A.L. Leal-Cruz and V. Ibarra-Junquera, Int. J. Surface Sci. Eng., 8 (2014) 71–91.
[9] I. Campos, M. Islas, G. Ramírez, C. VillaVelázquez and C. Mota, Appl. Surf. Sci., 253 (2007) 6226–6231.
[10] I. Campos, M. Islas, E. González, P. Ponce and G. Ramírez., Surf. Coat. Technol., 201 (2006) 2717–2723.
[11] R.D. Ramdan, T. Takaki and Y. Tomita, Mater. Trans., 49 (2008) 2625–2631.
[12] I. Campos, J. Oseguera, U. Figueroa, J.A. Garcıa, O. Bautista and G. Kelemenis, Mater. Sci. Eng. A, 352 (2003) 261–265.
[13] C.M. Brakman, A.W.J. Gommers and E.J. Mittemeijer, J. Mater. Res., 4 (1989) 1354–1370.
[14] O.A. Gómez-Vargas, M. Keddam and M. Ortiz-Domínguez, High Temp. Mater. Process., 36 (2017) 197–208.
[15] B. Mebarek, A. Benguelloula and A. Zanoun, Effect of Boride Incubation Time During the Formation of Fe_2B Phase, Mater. Res., (2017) Doi:http://dx.doi.org/10.1590/1980-5373-MR-2017-0647.
[16] M. Keddam, M. Elias-Espinosa, M. Ortiz-Domínguez, I. Simón-Marmolejo and J. Zuno-Silva, Int. J. Surf. Sci. Eng., 11 (2017) 563–585.
[17] M. Keddam, M. Ortiz-Dominguez, M. Elias-Espinosa, A. Arenas-Flores, J. Zuno-Silva, D. Zamarripa–Zepeda and O.A. Gomez-Vargas, Metallurgical Mater. Trans., 49 (2018) 1895–1907.
[18] L.G. Yu, X.J. Chen, K.A. Khor and G. Sundararajan, Acta Mater., 53 (2005) 2361–2368.
[19] M.G. Krukovich, B.A. Prusakov and I.G. Sizov, The Components and Phases of Systems 'Boron-Iron' and 'Boron-Carbon-Iron', Chapter Plasticity of Boronized Layers, Mater. Sci., 237 (2016) 13–21 Springer Series.
[20] H. Okamoto, J. Phase Equilib. Diffus., 25 (2004) 297–298.
[21] T.R. Goodman, Adv. Heat Transfer, 1 (1964) 51–122.
[22] H. Kunst and O. Schaaber, Harterei –Tech Mitt., 22 (1967) 275–292.
[23] E. Medvedovski, Adv. Eng. Mater., 18 (2016) 11–33.
[24] I.S. Dukarevich, M.V. Mozharov and A.S. Shigarev, Met. Sci. Heat Treat., 15 (1973) 160–162.
[25] G. Palombarini and M. Carbucicchio, J. Mater. Sci. Lett., 6 (1987) 415–416,.
[26] M. Kulka, N. Makuch, A. Pertek and L. Maldzinski, J. Solid. State. Chem., 199 (2013) 196–203.
[27] G. Kartal, O. Eryilmaz, G. Krumdick, A. Erdemir and S. Timur, Appl.Surf. Sci., 257 (2011) 6928–6934.
[28] S. Taktak, J. Mater. Sci., 41 (2006) 7590–7596.
[29] I. Uslu, H. Comert, M. Ipek, O. Ozdemir and C. Bindal, Mater. Des., 28 (2007) 55–67.
[30] I. Altinsoy, F.G. Celebi Efe, M. Ipek, I. Ozbek, S. Zeytin and C. Bindal, AIP Conf. Proc., 1569 (2013) 43–46.
[31] G. Palombarini and M. Carbucicchio, J. Mater. Sci. Lett., 3 (1984) 791–794.
[32] A.J. Ninham and I.M. Hutchings, J. Vac. Sci. Technol. A, 4 (1986) 2827–2831.
[33] G. Rodríguez-Castro, I. Campos-Silva, J. Martínez-Trinidad, U. Figueroa-López, I. Arzate-Vázquez, E. Hernández-Sánchez and J. Hernández-Sánchez, Kovove Mater., 50 (2012) 357–364.